

Thermogelling Biodegradable Polymers with Hydrophilic Backbones: PEG-*g*-PLGA

Byeongmoon Jeong,[†] Merinda R. Kibbey,[†] Jerome C. Birnbaum,[†]
You-Yeon Won,[‡] and Anna Gutowska^{*,†}

Pacific Northwest National Lab. (PNNL), 902 Battelle Boulevard, P.O. Box 999, K2-44, Richland, Washington 99352, and Department of Chemical Engineering and Materials Science, University of Minnesota, Minneapolis, Minnesota 55455

Received April 12, 2000; Revised Manuscript Received September 3, 2000

ABSTRACT: The aqueous solutions of poly(ethylene glycol) grafted with poly(lactic acid-*co*-glycolic acid) flow freely at room temperature but form gels at higher temperature. The existence of micelles in water at low polymer concentration was confirmed by cryo-transmission electron microscopy and dye solubilization studies. The micellar diameter is about 9 nm, and the critical micelle concentration is in a range of 0.01–0.05 wt %. The critical gel concentration, above which a gel phase appears, was 16 wt %, and the sol-to-gel transition temperature was slightly affected by the concentration between 16 and 25 wt %. At sol-to-gel transition, viscosity and modulus increased abruptly, and ¹³C NMR showed molecular motion of hydrophilic poly(ethylene glycol) backbones decreased while that of hydrophobic poly(lactic acid-*co*-glycolic acid) side chains increased. The hydrogel of PEG-*g*-PLGA with hydrophilic backbones was transparent during degradation and remained a gel for 1 week, suggesting a promising material for short-term drug delivery.

I. Introduction

Materials that gel in situ have recently gained attention as promising implantable drug delivery systems as well as injectable matrices for tissue engineering.^{1,2} In situ gelation is the basis of injectable systems that eliminate the need for surgical procedures and offers the advantage of the ability to form any desired implant shape. The change in molecular association can be driven by changes in temperature, pH, or solvent composition.^{3–7} Among the candidates of stimuli sensitive systems, organic solvent-free injectable systems are designed by using the thermosensitive sol-to-gel transition of aqueous solution. Such a system enables the pharmaceutical agents to be easily entrapped.

To perform as an ideal injectable system, the aqueous solution of a polymer should exhibit low viscosity at formulation conditions and gel quickly at physiological conditions. Considering the biomedical applications, the biocompatibility of the polymers is also an important issue. Therefore, the material should be biodegradable, and by keeping water-rich hydrogel properties, it should not induce tissue irritation during the degradation.

In situ gelling of aqueous Poloxamer 407 and *N*-isopropylacrylamide copolymers have been studied as candidate materials for injectable drug delivery systems and also tissue engineering applications.^{2,8} These materials are, however, nonbiodegradable, and animal studies demonstrated an increase in triglyceride and cholesterol after intraperitoneal injection of the aqueous Poloxamer 407 solution.⁹

Recently, Jeong et al. reported biodegradable, in situ gelling poly(ethylene glycol-*b*-(DL-lactic acid-*co*-glycolic acid)-*b*-ethylene glycol) (PEG-PLGA-PEG) triblock copolymers and poly((DL-lactic acid-*co*-glycolic acid)-*g*-

ethylene glycol) (PLGA-*g*-PEG) copolymers with hydrophobic PLGA backbones.^{10–12} They exhibited promising properties as an injectable drug delivery system. In vivo studies in rats demonstrated that the copolymer gels were still present after one month. During the degradation, the initially transparent gel became opaque due to preferential mass loss of hydrophilic PEG-rich segments. This change in morphology and the generation of an interface or phase might denature the protein drugs or cause cell deterioration in tissue engineering. In vitro release of porcine growth hormone (PGH) and insulin from the in-situ formed gel stopped after releasing 40–50% of loaded proteins.¹³

Certain drug formulations need a 1–2 week delivery system. For example, ifosfamide, a drug used for germ cell testicular cancer, is administered intravenously for five consecutive days. This treatment is repeated every 3 weeks or after recovery from hematological toxicity.¹⁴ To prepare such a short-term delivery system, poly(ethylene glycol) grafted with poly(lactic acid-*co*-glycolic acid) (PEG-*g*-PLGA), where hydrophilic PEG is a backbone, is designed. This material is expected to show a different gelation and degradation behavior and, consequently, a different drug release profile as compared to PEG-PLGA-PEG or PLGA-*g*-PEG.

II. Experimental Section

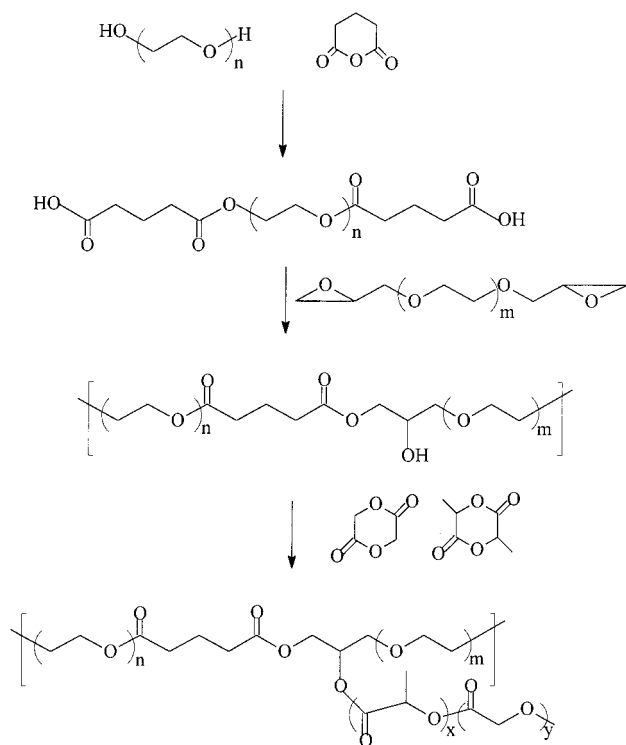
Materials. DL-Lactide (Polyscience) and glycolide (Polyscience) were recrystallized from ethyl acetate. Glutaric anhydride (Aldrich), glutaric acid (Aldrich), stannous octoate (Aldrich), epoxy-terminated poly(ethylene glycol) (MW: 600; Polyscience), poly(ethylene glycol) (MW:1000; Aldrich), and 1,6-diphenyl-1,3,5-hexatriene (DPH; Aldrich) were used as received.

Synthesis. PEG-*g*-PLGA was prepared according to Scheme 1. First, PEGs (MW = 1000, 38.28 g, 38.28 mmol) were dissolved in 90 mL of toluene. Toluene was then distilled off to a final volume of 50 mL to remove water by azeotropic distillation. Glutaric anhydride (7.255 g, 80.39 mmol) and glutaric acid (0.042 g, 0.40 mmol) were added, and the reaction

[†] Pacific Northwest National Lab.

[‡] University of Minnesota.

* To whom correspondence should be addressed. E-mail anna.gutowska@pnl.gov; Fax 509-375-2186; Tel 509-375-4443.

Scheme 1. Synthesis of PEG-*g*-PLGA

mixture was stirred at 120 °C for 6 h. Diethyl ether was added to the reaction mixture to precipitate out the carboxylic acid-terminated PEG (CPEG). The product was placed under high vacuum ($\sim 10^{-3}$ mmHg) for 48 h to remove the residual solvent. In the second step, epoxy-terminated PEG (EPEG) (MW = 600, 5.619 g, 9.36 mmol) was reacted with CPEG (11.50 g, 9.36 mmol) in toluene at 120 °C for 24 h to prepare PEG with pendant hydroxyl groups (PEGH) along the PEG backbone. In the third step, DL-lactide (19.2 g, 133.3 mmol) and glycolide (6.4 g, 55.1 mmol) were polymerized in situ on the preformed PEGH backbone at 130 °C for 24 h, using stannous octoate (76 μ L, 0.187 mmol) as a catalyst. The graft copolymers were precipitated into excess ethyl ether, and the residual solvent was removed under vacuum.

Gel Permeation Chromatography (GPC). The GPC system (Waters 515) with a refractive index detector (Waters 410) was used to obtain molecular weight and molecular weight distribution. The GPC data were calibrated with polystyrene standards with molecular weights in a range of 600–30 000. Styragel HMW 6E and HR 4E columns (Waters) were used in series. Tetrahydrofuran (THF) was used as an eluting solvent.

Cryo-Transmission Electron Microscopy (Cryo-TEM). Using cryo-TEM, a 1% PEG-*g*-PLGA solution was investigated in the form of vitreous films. Detailed procedures for the sample preparation have been published elsewhere.¹⁵ The liquid films of 10–300 nm thickness freely spanning across the micropores in a carbon-coated lacelike polymer substrate were prepared at 23.7 °C with complete control of temperature and humidity and rapidly vitrified with liquid ethane at its melting temperature (-180 °C). Imaging was performed using a JEOL 1210 operating at 120 kV. Adequate phase contrast was obtained at a nominal underfocus of ~ 6 μ m. Images were recorded on a Gatan 724 multiscan camera, and optical density gradients in the background were digitally corrected.

Cmc Determination. The hydrophobic dye 1,6-diphenyl-1,3,5-hexatriene (DPH) was dissolved in methanol with a concentration of 0.4 mM. This solution (20 μ L) was injected using a microsyringe into 2.0 mL of PEG-PLGA polymer aqueous solution with various concentrations between 0.0032 and 0.26 wt % and equilibrated for 5 h at 4 °C. A UV-vis spectrometer (HP 8453) was used to get the UV-vis spectra in the range 280–450 nm at 20 °C. The cmc was determined

by the plot of the difference in absorbance at 377 nm and at 391 nm ($A_{377} - A_{391}$) versus logarithmic concentration.

Viscosity. The viscosity of PEG-*g*-PLGA aqueous solution (22 wt %) was measured as a function of temperature. A Canon-Fenske viscometer 200 with a viscometer constant of 0.0966 cSt/s was used to measure the viscosity of the polymer solution.

Dynamic Mechanical Analysis. The sol-gel transition of the graft copolymer aqueous solution (22 wt %) was investigated using a dynamic mechanical rheometer (Rheometric Scientific: SR 2000). The polymer solution was placed between parallel plates having a diameter of 25 mm and a gap distance of 0.5 mm. The data were collected under controlled stress (4.0 dyn/cm²) and frequency of 1.0 rad/s.¹⁶ The heating and cooling rate was 0.2 °C/min.

Sol-Gel Transition. The sol-gel transition was determined by a test tube inverting method with a temperature increment of 1 °C per step.¹⁷ Polymer aqueous solutions (0.5 g) were prepared in 4 mL vials with inner diameters of 11 mm. The vials were immersed in a water bath at each step for 15 min. The sol-gel transition temperature was monitored by inverting the vials, and if there was no flow in 30 s, it was regarded as a gel. The transition temperature was determined with ± 1 °C accuracy.

NMR Study. A NMR spectrometer (Varian VXR 300) was used for ¹H NMR and ¹³C NMR to study composition and microenvironment change during sol-to-gel transition. For the ¹³C NMR in D₂O, a 22 wt % PEG-*g*-PLGA solution was prepared.

III. Results and Discussion

Synthesis. PEG-*g*-PLGA was synthesized by three steps as shown in Scheme 1.

Carboxylic acid-terminated PEG (CPEG) was prepared by reacting PEG with excess amount of glutaric anhydride in the presence of catalytic amounts of glutaric acid. Formation of the compound was confirmed by ¹H NMR in CDCl₃. The chemical shifts (ppm) in the spectra are 1.9 (central methylene of glutarate), 2.4 (methylene of glutarate next to carbonyl group), 3.6 (ethylene of PEG), and 4.2 (methylene of PEG connected to glutarate). The one to one area ratio of the peaks at 1.9 and 4.2 ppm indicates the quantitative end group functionalization.

PEG with hydroxy pendant groups (PEGH) was prepared by the reaction of CPEG and epoxy-terminated PEG (EPEG). The weight-average molecular weight (M_w) and polydispersity index (PDI) of resulting PEGH, which were determined by GPC, was 3000 and 1.3 relative to polystyrene standards. The peaks at 1.9 and 2.4 ppm come from glutarate. The peaks at 3.6 and 4.3 ppm come from PEG. The small overlapped peaks 3.4–4.2 ppm of PEGH come from the connecting methylene or methine moieties between CPEG and EPEG (Scheme 1). It is hard to conclude the precise structure of PEGH based on ¹H NMR data. There are two possibilities of the ring-opening pattern of the epoxy group during the reaction of EPEG and CPEG. The nucleophiles prefer to attack the sterically less hindered side of the epoxy group in the base-catalyzed addition, while ring-opening is less regiospecific in cationic polymerization.¹⁸ The GPC chromatogram in Figure 2 shows the increase in molecular weight by the formation of PEGH from CPEG and EPEG. Assuming a PEGH molecular weight of about 3000, there are ~ 2 –3 pendant hydroxy groups per each PEGH.

The resultant PEGH was used as an initiator for the ring-opening polymerization of DL-lactide and glycolide in the presence of stannous octoate as a catalyst. ¹H

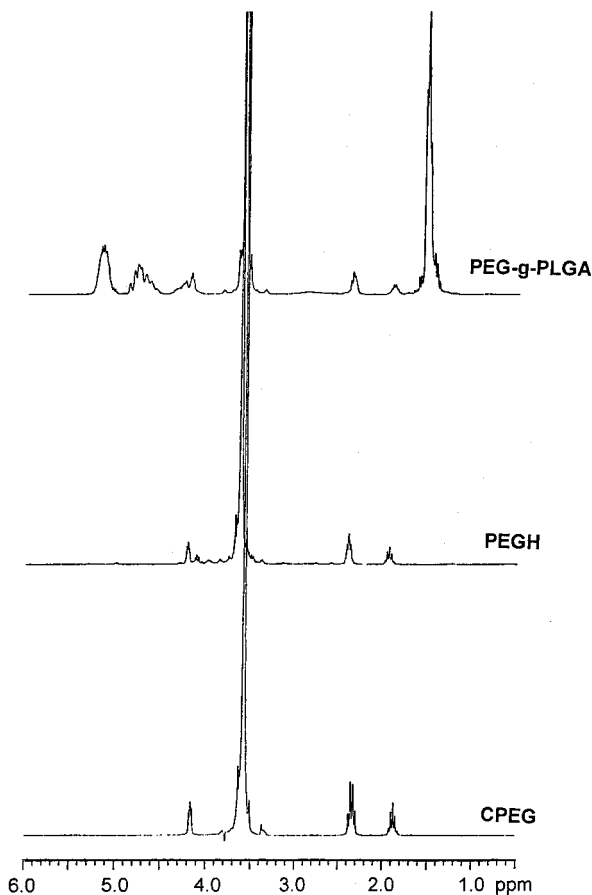


Figure 1. ^1H NMR of CPEG, PEGH, and PEG-*g*-PLGA in CDCl_3 . CPEG, PEGH, and PEG-*g*-PLGA indicate carboxylic acid-terminated PEG (first step), PEG with pendant hydroxy groups (second step), and PEG grafted with PLGA (third step), respectively.

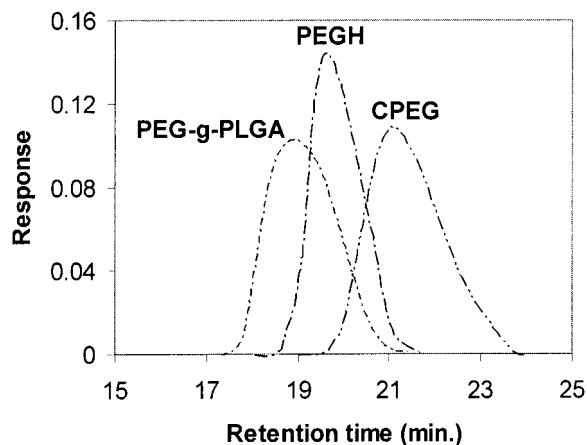


Figure 2. GPC chromatogram of polymers showing progress of reactions. CPEG, PEGH, and PEG-*g*-PLGA indicate carboxy-terminated PEG (first step), PEG with pendant hydroxy groups (second step), and PEG grafted with PLGA (third step).

NMR spectra show an ethylene glycol unit at 3.6 ppm, a lactic acid unit at 5.3 ppm (methine) and 1.8 ppm (methyl), and a glycolic acid unit at 4.8 ppm. Composition of the PEG-*g*-PLGA calculated by ^1H NMR was 2.98/2.35/1.00 (ethylene glycol/DL-lactic acid/glycolic acid) in mole ratio. The methylene protons of the epoxy group show up at 2.6 and 2.8 ppm in ^1H NMR. In the ^1H NMR spectrum of PEGH and PEG-*g*-PLGA the epoxy signals are too small to be analyzed quantitatively. Weight-average molecular weight (M_w) and PDI of PEG-*g*-PLGA

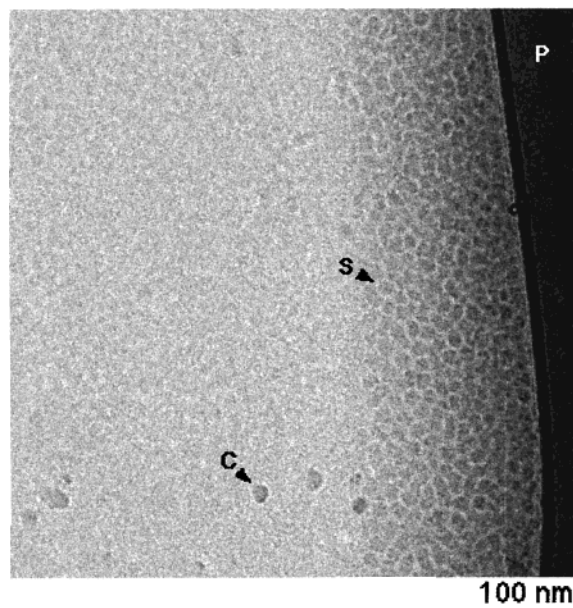


Figure 3. Cryo-TEM image showing micelle formation of the PEG-*g*-PLGA polymer at a concentration of 1 wt % in water at 23.7 °C. P, C, and S denote the substrate carbon-polymer film, ice condensates, and spherical micelles, respectively. The spheroidal micelles are preferentially collected around the edge of the sample film because the thickness is greater there than in the center.

determined by GPC were 6000 and 1.5 relative to polystyrene standards.

Micellization. PEG-*g*-PLGA is an amphiphilic copolymer, and a core-shell structure can be expected in water. The hydrophobic PLGA side chains form a core, and the hydrophilic PEG backbones form a shell region. The formation of core-shell structure was investigated by cryo-transmission electron microscopy (cryo-TEM)^{19,20} and the dye solubilization method.²¹

The formation of micelles was directly confirmed by a cryo-TEM image. A 1 wt % PEG-*g*-PLGA solution at 23.7 °C was quenched into a vitrified form at -180 °C. The cryo-TEM image shows closely packed spherical micelles (denoted as S in Figure 3) on the left side of black stripe. The diameter of a micelle is about 9 nm.

At a fixed concentration of DPH, the polymer concentration was increased from 0.0032 to 0.26 wt %. The absorption coefficient of the hydrophobic dye (DPH) is much higher in a hydrophobic environment than in water. Thus, with increasing polymer concentration, the absorbance at 377 and 356 nm increased, indicating that the polymers formed a core-shell structure in water creating a hydrophobic environment (Figure 4a). The critical micelle concentration (cmc) was determined by extrapolating the absorbance at 377 nm minus absorbance at 391 nm ($A_{377} - A_{391}$) versus logarithmic concentration (Figure 4b) to compensate for the scattering effect. The cmc value determined by this extrapolation is not precise due to the uncertainty in the line, but it is in a range of 0.01–0.05 wt % at 20 °C.

Sol-Gel Transition. At high concentrations, the PEG-*g*-PLGA aqueous solution undergoes a sol-to-gel transition with increasing temperature. The viscosity of a 22 wt % PEG-*g*-PLGA aqueous solution that was measured by a Cannon-Fenske viscometer was 27 cP at 20 °C. This viscosity is low enough for an easy formulation of the polymer with pharmaceutical agents that could be injected using a 22 gauge needle. Above

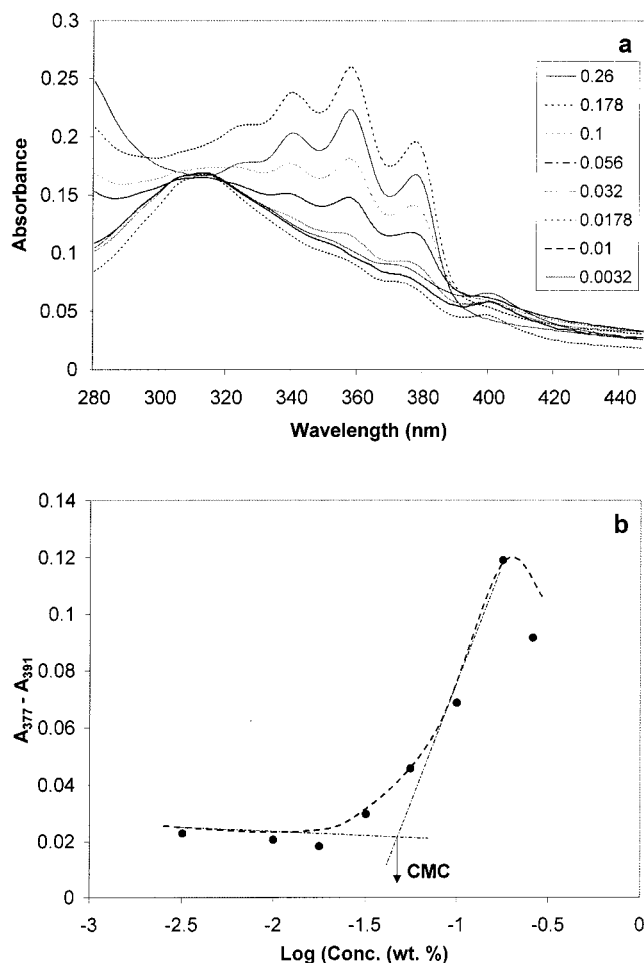


Figure 4. (a) UV spectra showing the formation of core-shell structure of polymers in water at 20 °C. DPH concentration was fixed at 4 μM and polymer concentration varied: 0.0032, 0.01, 0.0178, 0.032, 0.056, 0.10, 0.178, and 0.26 wt %. The increase in absorption band at 377 nm with increasing polymer concentration indicates the formation of a hydrophobic environment, that is, micelles, in water. (b) The cmc determination by extrapolation of the difference in absorbance at 377 and 391 nm.

the gelation temperature, the viscosity is too high to flow through the capillary of this viscometer. Dynamic mechanical analysis of 22 wt % aqueous polymer solutions shows that the real part (η') of complex viscosity increases from 5 to 500 $\text{dyn}\cdot\text{cm}^{-2}$ [P] and elastic modulus (G') increased from 0 to 100 $\text{dyn}\cdot\text{cm}^{-2}$ during a sol-to-gel transition (Figure 5). η' and G' are measures of dissipated energy and stored energy, respectively, when a material is subject to cyclic deformation. And, practically no flow was observed above 30 °C in the test tube inverting method, indicating a sol-to-gel transition. When we compare the two methods for 22 wt % aqueous polymer solutions, the gelation temperature determined by a test tube inverting method corresponds to the temperature at which η' of 100 P and G' of 50 dyn/cm^2 are reached in dynamic mechanical analysis when thermal equilibrium is assumed in both cases.

The phase diagram of PEG-*g*-PLGA aqueous solutions determined by a test tube inverting method is shown in Figure 6. The sol-to-gel transition is accompanied by a sharp increase in viscosity. The critical gel concentration (cgc) above which the gel phase appears was about 16 wt %. Below cgc, the system flows even though the viscosity increases as the temperature increases. The

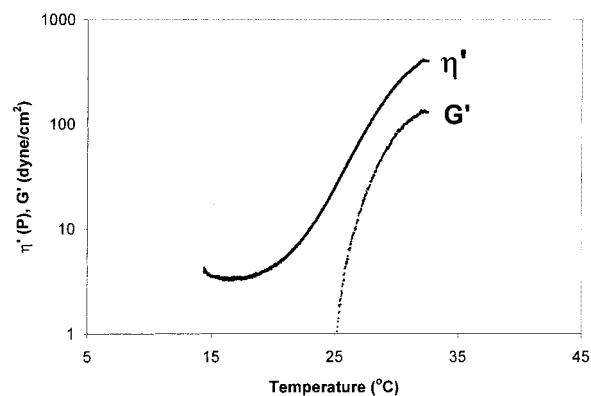


Figure 5. Real part (η') of complex viscosity and elastic modulus (G') of 22 wt % PEG-*g*-PLGA aqueous solutions as a function of temperature. Below 25 °C, G' is negligible because the system is a low viscous sol. With increasing temperature, the viscosity and modulus increase abruptly to undergo a sol-to-gel transition at around 30 °C.

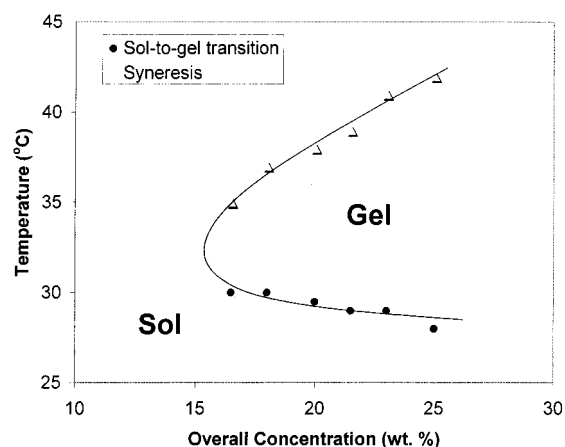


Figure 6. Phase diagram of PEG-*g*-PLGA aqueous solution. The concentration is the overall concentration of polymers in water. Filled circles and gray triangles indicate sol-to-gel transition and syneresis. The gel region, right side of trend line, is the region where the uniform gel phase exists.

sol-to-gel transition temperature, estimated at about 30 °C, was slightly affected by the polymer solution concentration. The presence of the gel phase around body temperature (37 °C) indicates that the material is a promising candidate for an injectable drug delivery system that can be formulated at room temperature and would form a gel in situ upon subcutaneous or intramuscular injection. The pharmaceutical agents would then be slowly released from the in situ formed gel.

Further analysis of the phase diagram illustrates that with increasing temperature the gel exhibits syneresis, marked as gray triangles in Figure 6, a macromolecular phase separation where some amount of water is exuded from the gel phase. Above the syneresis temperature, the gel phase remains separated from the water. Therefore, the sol phase at low temperature is a homogeneous one-phase solution while the sol phase above syneresis is a two-phase system. The gel region, right side of the trend line in the phase diagram, indicates the area where a uniform gel phase exists. On the basis of the phase diagram, 21–25 wt % of PEG-*g*-PLGA aqueous solutions are recommended as injectable formulations for drug delivery.

The aggregation number of a micelle can be estimated from the size of the micelle by assuming that the micelle is a hard sphere. The radius of a micelle can be

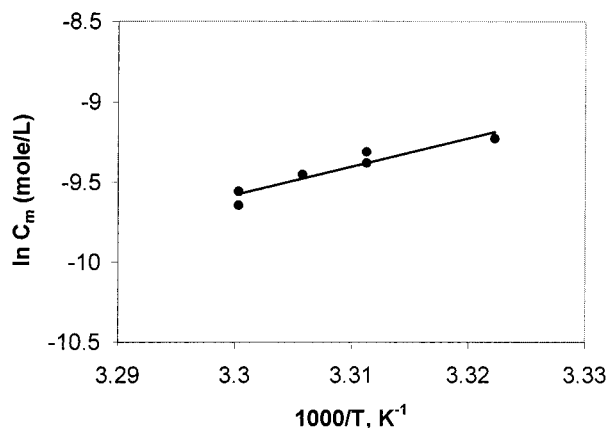


Figure 7. Calculation of enthalpy of sol-to-gel transition of PEG-*g*-PLGA aqueous solutions.

estimated from eq 1.^{22,23}

$$R = (3M_{SD}v_2/4\pi N_A)^{1/3} \quad (1)$$

where M_{SD} denotes the molecular weight of a micelle obtained from centrifugal sedimentation which is close to weight-average molecular weight (M_w). v_2 and N_A are the partial specific volume of the polymer and Avogadro's number, respectively.

The aggregation number of a micelle (N_{ag}) is given by eq 2.

$$N_{ag} = M/M_0 \quad (2)$$

where M and M_0 denote molecular weight of a micelle and molecular weight of a polymer, respectively. Assuming v_2 is 0.95, which is typical for polyester or polyether,²² and R is about 4.5 nm (diameter \sim 9 nm) from cryo-TEM, the micellar aggregation number is 40 at 20 °C. The aggregation number of a micelle is assumed to be practically constant for a sol region as in the cases of PEG-PLGA-PEG and Poloxamer 407.^{24,25} This calculation also assumes that M is equal to M_{SD} , and the molecular weight of PEG-*g*-PLGA (M_0) is 6000 as determined from GPC data.

On the basis of this estimation, the thermodynamic functions such as enthalpy (ΔH^0), Gibbs free energy (ΔG^0), and entropy of gelation (ΔS^0) can be calculated.²⁶ Now, the standard states of gelation process are taken to be the micelles in ideal dilute solution at unit molarity and micelles in gel state.

$$\Delta G^0 = RT_{gel} \ln C_m \quad (3)$$

$$\Delta H^0 = R[d \ln C_m / d(1/T_{gel})] \quad (4)$$

$$\Delta S^0 = (\Delta G^0 - \Delta H^0) / T_{gel} \quad (5)$$

C_m is the concentration of micelles in mol L⁻¹ that is calculated by assuming that the aggregation number per micelle is 40. T_{gel} is the sol-to-gel transition temperature. ΔH^0 calculated from the slope of $\ln C_m$ versus $1/T_{gel}$ (Figure 7) is 146 kJ mol⁻¹ (micelle) or $\Delta H^0 = 3.65$ kJ mol⁻¹ (chain). This value is similar to gelation of poloxamer 407 ($\Delta H^0 = 1.5$ kJ mol⁻¹ (chain)) and PEG-PLGA-PEG triblock copolymers ($\Delta H^0 = 1.32$ kJ mol⁻¹ (chain)).^{27,28} Gibbs free energy (ΔG^0) and entropy (ΔS^0) for the gelation of 22 wt % PEG-*g*-PLGA aqueous solution with a T_{gel} of 30 °C are -0.59 kJ mol⁻¹ and 1.9

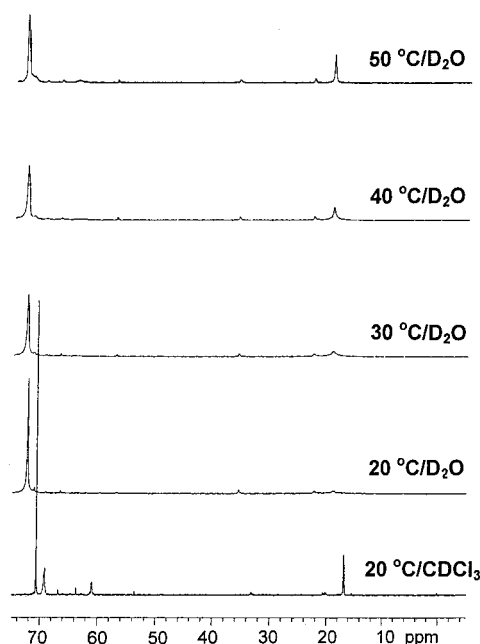


Figure 8. ¹³C NMR spectra of PEG-*g*-PLGA in D₂O (22 wt %) as a function of temperature. The ¹³C NMR spectrum in CDCl₃ is also shown as a reference.

J mol⁻¹ K⁻¹, respectively. This calculation leads to the conclusion that the gelation is driven by the entropy. The molecular origin of such an entropy-driven process has been suggested as hydrophobic interactions.²⁹ Water molecules tend to surround the hydrophobic segment (PLGA) to decrease the free energy. Consequently, the entropy of water molecules decreases in the presence of hydrophobes. Therefore, the surface area of hydrophobic molecules is minimized in water. Such hydrophobic interactions increase with increasing temperature, change the molecular conformation of PEG-*g*-PLGA, and thus might drive the gelation.³⁰

The ¹³C NMR analysis of the polymers was conducted at different temperatures to elucidate the structure of the gel and mechanism of gel formation (Figure 8). Spectra of polymers dissolved in water and chloroform were compared. The ¹³C NMR spectra of a 22 wt % PEG-*g*-PLGA in D₂O were obtained at 20 (sol state), 30 (just above sol-to-gel transition), 40 (gel state), and 50 °C (macrophase-separated state) by simply increasing the temperature around the probe without changing NMR parameters. The equilibration time at each temperature was 15 min. Chloroform (CDCl₃) is a nonselective good solvent for both PEG and PLGA blocks while water (D₂O) is a good solvent for PEG but is a poor solvent for PLGA. The sharp peaks of both PEG and PLGA in chloroform are compared with a collapsed peak of PLGA in water at first and second rows of ¹³C NMR, indicating core (PLGA)-shell (PEG) structure of the polymer in water. The molecular motion of PEG in water is decreased due to anchoring effects by the hydrophobic PLGA segments compared with that in chloroform. This fact is reflected in a broadened peak of PEG in D₂O at 20 °C. The change in molecular association at sol-to-gel transition involves the change in molecular motion of the polymers. The change in ¹³C NMR with increasing temperature (20–50 °C) shows such a change in microenvironment around the PEG and PLGA. The PEG peak (72 ppm) at a gel state (30 °C) is broadened and decreased by half in height compared with a sol state (20 °C), whereas there is a slight increase in PLGA peak

height (20 ppm) at gel state (30 °C). These changes in peak heights indicate a significant decrease in molecular motion of the PEG backbone and increased thermal motions of the PLGA side chains during the sol-to-gel transition. This behavior is quite different from that of PLGA-*g*-PEG. PLGA-*g*-PEG showed little change in PEG peak during the sol-to-gel transition at ¹³C NMR in D₂O.¹² On the basis of these observations, the following model can be suggested for the sol-to-gel transition of PEG-*g*-PLGA copolymer aqueous solutions. In a sol state, the polymer conformation is micellar where the PEGs occupy shell and PLGAs occupy core of the micelle. The degree of association in a sol state is not enough to form a three-dimensional network. With increasing temperature, the hydrophobic interactions increase and associations of polymers decrease the PEG molecular motion, resulting in a long-range network formation, that is, a gel. The degree of association is strong enough to keep its integrity in the presence of excess water at a given temperature such as 37 °C. Therefore, we can define this system as a gel rather than a solution with an increased viscosity. As the temperature increases further, the long-range interactions among the polymers increase, and phase mixing between PEG and PLGA occurs,³¹ resulting in the macrophase separation between water and polymer that occurs at 50 °C.

The 22 wt % polymer solutions (0.5 g) are injected into 4 mL vials (diameter of 1.1 cm) and kept in a 37 °C water bath for 5 min. During this time the gel forms. A 3 mL aliquot of phosphate buffer saline (37 °C, pH = 7.4) is added, and the vials are shaken (16 strokes/min) in the water bath to simulate body conditions. The gel keeps its integrity for 1 week in vitro, and the initially turbid gel becomes transparent in 3–7 days. After 7 days, the gel totally disintegrated to become a clear polymer solution.

This material can be applied for a short-term delivery of pharmaceutical agents such as proteins and anticancer drugs. The hydrophobicity of the drug and the molecular structure of the polymers affect the extent of diffusion or degradation dominant drug release profile.¹⁰ Therefore, by choosing the appropriate drug and molecular parameters of PEG-*g*-PLGA, a short-term delivery system can be designed on the basis of this polymer hydrogel.

IV. Conclusions

The aqueous solutions of PEG-*g*-PLGA copolymers exhibited a sol-to-gel transition in response to an increase in temperature. Micelle formation was confirmed by cryo-TEM and the dye solubilization method. The micellar diameter was about 9 nm, and the cmc was in the range 0.01–0.05 wt %. ¹³C NMR shows that the molecular motion of PEG backbones decreases while that of PLGA side chains increases during the sol-to-gel transition.

The 21–25 wt % solutions exhibit low viscosity at room temperature and form gels at body temperature. The gel morphology changed from turbid to transparent,

and the integrity of gel persisted for 1 week, suggesting a promising candidate for short-term drug delivery systems.

Acknowledgment. This work was supported by Battelle Independent Research and Development funds.

References and Notes

- (1) Hill-West, J. L.; Chowdhury, S. M.; Slepian, M. J.; Hubbell, J. A. *Proc. Natl. Acad. Sci. U.S.A.* **1994**, *91*, 5967–5971.
- (2) Stile, R. A.; Burghardt, W. R.; Healy, K. E. *Macromolecules* **1999**, *32*, 7370–7379.
- (3) Chen, G. H.; Hoffman, A. S. *Nature* **1995**, *373*, 49–52.
- (4) Thomas, J. L.; You, H.; Tirrell, D. *J. Am. Chem. Soc.* **1995**, *117*, 2949–2950.
- (5) Malstom, M.; Lindman, B. *Macromolecules* **1992**, *25*, 5446–5450.
- (6) Yang, J.; Pickard, S.; Deng, N. J.; Barlow, R. J.; Attwood, D.; Booth, C. *Macromolecules* **1994**, *27*, 670–680.
- (7) Jeong, B.; Bae, Y. H.; Lee, D. S.; Kim, S. W. *Nature* **1997**, *388*, 860–862.
- (8) Johnston, T. P.; Punjabi, M. A.; Froelich, C. *J. Pharm. Res.* **1992**, *9* (3), 425–434.
- (9) Wout, Z. G. M.; Pec, E. A.; Maggiore, J. A.; Williams, R. H.; Palicharla, P.; Johnston, T. P. *J. Parenter. Sci. Technol.* **1992**, *46* (6), 192–200.
- (10) Jeong, B.; Bae, Y. H.; Kim, S. W. *J. Controlled Release* **2000**, *63*, 155–163.
- (11) Jeong, B.; Bae, Y. H.; Kim, S. W. *J. Biomed. Mater. Res.* **2000**, *50* (2), 171–177.
- (12) Jeong, B.; Gutowska, A. *J. Am. Chem. Soc.*, submitted.
- (13) Jeong, B. Unpublished data.
- (14) IFEX Prescription, <http://www.ifex.com/ifu.html>, A Bristol-Meyers Squibb Co., Princeton, NJ 08543.
- (15) Bellare, J. R.; Davis, H. T.; Scriven, L. E.; Talmon, Y. J. *Electron Microsc. Technol.* **1988**, *10*, 87–111.
- (16) Wanka, G.; Hoffmann, H.; Ulbricht, W. *Colloid Polym. Sci.* **1990**, *268*, 101–117.
- (17) Tanodekaew, S.; Godward, J.; Heatley, F.; Booth, C. *Macromol. Chem. Phys.* **1997**, *198*, 3385–3395.
- (18) Odian, G. In *Principles of Polymerization*, 2nd ed.; John Wiley & Sons, Inc. Korean Student Ed.: Korea, 1981; p 513.
- (19) Alexandridis, P.; Holzwarth, J. F.; Hatton, T. A. *Macromolecules* **1994**, *27*, 2414–2425.
- (20) Discher, B. M.; Won, Y.-Y.; Ege, D. S.; Lee, J. C. M.; Bates, F. S.; Discher, D. E.; Hammer, D. A. *Science* **1999**, *284*, 1143–1146.
- (21) Won, Y.-Y.; Davis, H. T.; Bates, F. S. *Science* **1999**, *283*, 960–963.
- (22) Brown, W.; Schillen, K.; Almgren, M.; Hvidt, S.; Bahadur, P. *J. Phys. Chem.* **1991**, *95*, 1850–1858.
- (23) Cau F.; Lacelle, S. *Macromolecules* **1996**, *29*, 170–178.
- (24) Jeong, B.; Bae, Y. H.; Kim, S. W. *Colloids Surf. B: Biointerfaces* **1999**, *16*, 185–193.
- (25) Zhou, Z.; Chu, B. *J. Colloid Interface Sci.* **1988**, *126*, 171–180.
- (26) Deng, Y.; Yu, G. E.; Price, C.; Booth, C. *J. Chem. Soc., Faraday Trans.* **1992**, *88*, 1441–1446.
- (27) Yu, G. E.; Deng, Y.; Dalton, S.; Wang, Q. G.; Attwood, D.; Price, C.; Booth, C. *J. Chem. Soc., Faraday Trans.* **1992**, *88*, 2537–2544.
- (28) Jeong, B.; Bae, Y. H.; Kim, S. W. *Macromolecules* **1999**, *32*, 7064–7069.
- (29) Israelachvili, J. N. *Intermolecular and Surface Forces*; Academic Press: New York, 1985.
- (30) Feil, H.; Bae, Y. H.; Feijen, J.; Kim, S. W. *Macromolecules* **1993**, *26*, 2496–2500.
- (31) Jeong, B.; Lee, D. S.; Shon, J. I.; Bae, Y. H.; Kim, S. W. *J. Polym. Sci., Polym. Chem.* **1999**, *37*, 751–760.

MA000638V